Indian Journal of Engineering & Materials Sciences
Vol. 28, February 2021, pp. 5-20

Friction stir processing of aluminum alloys

Pratap Singh* & Hans Raj Kandikonda
Faculty of Engineering, Dayalbagh Educational Institute, Dayalbagh, Agra 282 005, India

Received: 31 August 2020; *Accepted: 4 February 2021*

In most of the industries like automobile, aircraft, shipbuilding, etc., surface composites play an important role as they enhance strength, hardness, and microstructure. Friction Stir Processing is a solid-state surface alteration and surface engineering technique employed for development of Metal Matrix Composite surfaces. It enables alteration of the surface, control of microstructure, enhancement of wear and improvement in mechanical properties. This process was first initiated with Al-based alloys for enhancing their mechanical properties and now extended to the fabrication of various other alloys also such as Mg, Ti, Cu, etc. An effort is made in this article to review the current trends and future scope of Al alloy composites using FSP including various FSP strategies applied to improve surface characteristics, hardness, microstructure, enhancement of wear.

Keywords: Friction stir processing, Composite material, Aluminum alloy

1 Introduction

Metal Matric Composites (MMCs) are composite materials with a combination of at least two components, base metal/alloy, and a hard ceramic. A fabrication of MMC is usually done by dispersing a reinforcement material into a metal matrix using various techniques. It includes casting[1–3], spray deposition[4–6], laser technique[7,8], powder metallurgy[9–11], electron beam irradiation[12,13], etc. All such techniques of composite fabrication are usually done at high temperatures in the liquid phase. During last two decades FSP gained popularity on account of ease with which it creates MMCs at low temperatures. FSP is normally conducted below the melting point and produces a good surface modification and is used for creation of bulk composites of metal alloys. The first journal paper based on FSP was published in 1999[14], and thereafter many papers and even patents appeared on this topic. The FSP was initially applied on wrought aluminum alloys for refinement of grains to provide super-plasticity[14], microstructure improvement of casting materials[15], and composites[16]. FSP can fabricate MMCs along the surface of the plate by Reinforcement Particles (RPs) and base metal alloys[17]. This is done by drilling blind holes or making grooves into the specimen which are then filled by reinforcement materials. The composites with nano-sized RPs produce high strength and uniform dispersion of particles[18]. The selection of the base material is important, because some materials may get softened during FSP, which nullify the benefits of incorporating RPs[19].

Nanoparticles offer high strengthening benefits in the fabrication of nano-composites. Dispersion of such particles is found to result in improvement of tensile strength and microhardness[20–22]. The operational steps of the FSP technique are shown in Fig. 1 (a). The FSP rotating tool consists of a shoulder and pin, the tool is inserted into the specimen up to a certain depth and then made to traverse along the specified path (Fig. 1 (b)). On account of the friction between the rotating shoulder and specimen, enough heat is generated which is utilized to soften the material. The rotating pin or probe stirs this heated material into the stir zone. The stir material drifts around the rotating tool and is exposed to severe plastic deformation, due to which, microstructure is refined in the stir zone and enhancement of mechanical properties takes place. When the tool moves ahead in processing direction, the cavity at the hindmost end fills by the stirred material of base alloy and reinforcement material[19–23].

A detailed description of process variables, reinforcement variables, and the influence of RPs is given below.

2 Process variables

FSP process variables can be divided into three categories namely, machine variables, tool variables and material properties (Fig. 2).

*Corresponding author (E-mail:pratapsingh@dei.ac.in)

2.1 Influence of machine variables

Rotational speed, traverse speed, and tool tilt angle are the major parameters. For aluminum alloys, rotational speed of 1200 rpm with traverse speed of 50 mm/min is mostly used. Machine variables can be easily controlled by altering the parameters through the machine settings. These parameters affect the refinement of the microstructure and mechanical properties of the processed specimen. Selection of higher rotational speed and lower travel speed leads to better dispersion of RPs, enhancement of heat, and material flow[24–26]. Axial force should be optimized to achieve a better distribution of particles. Low axial force leads to homogeneous distribution, while high force causes the ejection of particles during processing[19,27]. The tool plunge depth and tilt angle depth are interdependent. When the tool tilt angle increases by keeping plunge depth constant, the lesser surface of the shoulder touches the specimen results in less heat generation. In the study of Asadi *et al.*[28], plunge depths required are 0.22 mm, 0.30 mm, and 0.40 mm respectively for tilt angles of 2.5º, 3º, and 3.5º.

2.2 Influence of tool variables

The heat generated in the stir zone is primarily due to the friction between the tool and the work piece. This heat is generated due to plastic deformation of the material in the processed zone[23]. Designing of tools consists of shoulder design and pin design. Shoulder design consists of tool diameter and end

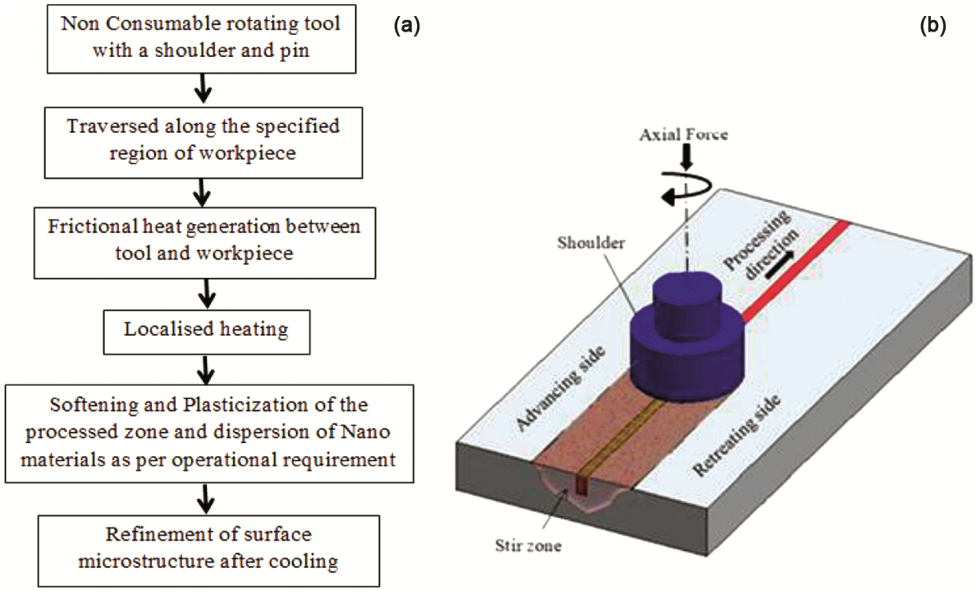

Fig. 1 — (a) FSP operational steps and (b) Schematic illustration of FSP.

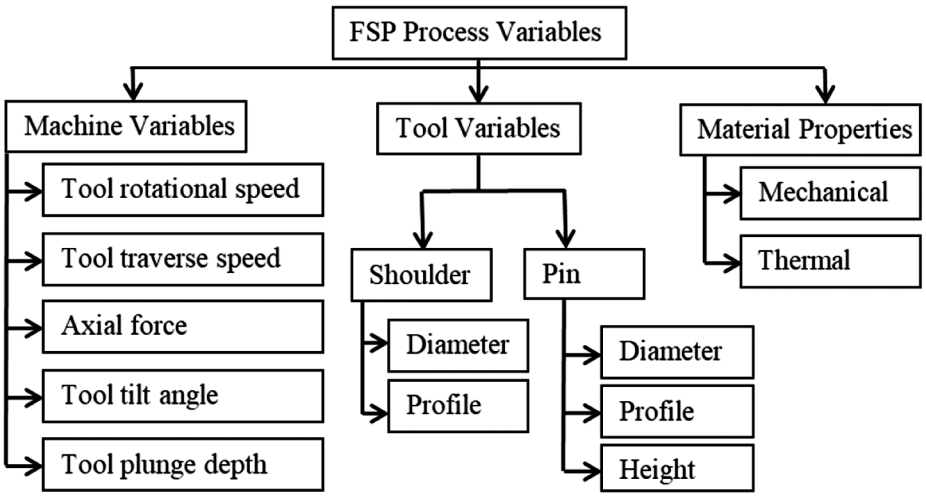

Fig. 2 — FSP process variables.

surface angle of the shoulder. Tool pin variables are pin diameter, length of the pin, and shape of the pin. Naresh Parumandla and Kumar Adepu[29] studied the effect of tool shoulder geometry on the mechanical properties and microstructure of the composites and found a defect free composite produced by using shoulder diameter of 24 mm at rotational speed of 1150 rpm and traverse speed of 15 mm/min while by using 21 mm shoulder diameter at the same conditions, micro cracks were observed. Experimental studies indicated that with the decrease of shoulder diameter from 24 mm and subsequent reduction in the pin diameter reduced material flow towards the weld cavity and increased the number of defects in the fabrication. For obtaining optimal properties, the ratio of three is generally used for shoulder to pin diameter[30,31]. Vijayavel *et al.*[32] reported that the value of three as a ratio of shoulder to pin diameter exhibited better microstructure and mechanical properties in the processed specimen. The end surface shape also affects the flow of material during friction stir processing. The end shoulder design consists of flatness, concavity, and convexity of shape as shown in Fig. 3. During processing with a flat surface, excessive flash is found because of larger surface contact between shoulder and work piece. In the case of concave shape, the stirred material lodged in the cavity under the shoulder causes the tool to lift upwards.

The pin design is also important. The pin profile affects the distribution of RPs and the flow of material. The tool pin or probe profile consists of various shapes and features such as flats, flutes, and threads (Fig. 4). John *et al.*[33] studied the influence of tool pin and found that the hexagonal tool pin profile exhibited higher ultimate tensile strength and yield strength in the work piece as compared to tools with other profiles. In some studies, it was found that a square pin produced a better quality distribution of particles as compared to circular and triangular shapes[34]. The square pin profiles result in better refinement of grains as compared to non-threaded circular probes[35]. The better dispersion of RPs and higher homogeneity are found in a tool having threaded pin profile as compared to square and cylindrical pins[36].

Fig. 3 — Different shoulder end surfaces.

2.3 Material properties

In the selection of process parameters, material properties play a key role. The thermal conductivity and shear affect the mechanical properties of the materials. In literature, various authors conducted experiments by considering various process parameters, selecting various types of reinforcement materials, by using multiple strategies for fabrication of composite. The effect of various reinforcement strategies on microstructure and mechanical properties is explained in Table 1.

3 Reinforcement variables

The categorization based on reinforcement variables is given below:

i. Type of Reinforcement Particles (RPs)
ii. Size and volume % of RPs
iii. Strategy of reinforcement

3.1 Type of reinforcement particles

Various types of RPs are reported in literature. These are aluminum oxide (Al_2O_3)[37–41], silicon carbide (SiC)[42–48], titanium oxide(TiO2)[49], boron carbide (B_4C)[50], tungsten carbide (WC)[51], titanium carbide (TiC)[52], zirconium aluminide (Al_3Zr)[53], Al_2Cu[54], nickel, titanium and copper (Ni,Ti,C)[55], Multi-Walled Carbon Nano Tubes (MWCNTs)[56], etc. The selection of reinforcement depends on compatibility with base metal and its end use application. Normally hybrid composites have two or more RPs at different volume fraction[55,57].

Fig. 4 — Different shapes of probe profile used in FSP.

Table 1—Summary of various features of FSP: dimensions of specimen used, tool material, tool geometry, process parameters and techniques used in fabrication of aluminium alloy and its composites.

(SD: Shoulder Diameter; PD: Pin Diameter; PL: Pin Length; AF: Axial Force, TPD: Tool Plunge Depth; EDM: Electric Discharge Machine).

Material of the specimen and its size in mm (L-Length, W-Width, T-Thickness	Tool material and its geometry (All dimensions are in mm)	FSP operational parameters (rotational speed, traverse speed, tool tilt angle, axial force)	Reinforcement type, its size and techniques (groove dimension: width × depth)	No. of Passes	Prominent Remarks
AA1050 (150L, 100W, 10T)	H13, SD-20, PD-6, PL-5	1180 rpm, 80 mm/min, 3º, plunge depth - 0.3 mm	Al_2O_3, Groove (1×3 mm^2)	2	Agglomeration of particles was found after the first FSP pass. Enhancements of tensile strength, wear resistance, homogeneity in microstructure, and better nanoparticle distribution was observed with the second pass FSP[37].
Al5083 (6.35T)	H13 steel tool, square pin, 5mm diagonal, PL- 4mm, concave shoulder, SD-18mm	710 rpm, 100mm/min, 2.5º	Al_2O_3, 75 µm, BlindHoles at a distant of 1 mm with diameter – 2 mm, depth – 2 mm, volume % ofRPs - 0.12 %	4	Wear resistance increases with an increase in rotational speed. SC fabricated in high heat input conditions results in higher hardness and defect-free stir zone[38].
Al6061 (4T)	Taper cylindrical threaded concave shoulder tool, concave radius-3.5, SD-24, PD-8 and 6, PL-3.8,	1150 rpm, 15 mm/min, 2.5º, AF-5 KN	Al_2O_3, 40 - 50 nm, Groove, 2 to 6 volume % of reinforcement with increment of 2	1	By increasing the volume %, microhardness increases while yield stress, UTS, and % of elongation decreases[39].
A356 (250L, 50W, 10T)	H13, SD-18, PD-3.6, PL-4, threaded pin	1600 rpm, 200 mm/min, 2º	A356/Al_2O_3 composite powder, 25-63 µm, High Velocity Oxy-Fuel (HVOF) Spraying	1	Homogeneous distribution and good bonding of particles with the Al matrix. Increase in microhardness andstrength[40].
Al2024 (120L, 50W, 4T)	H13, SD-18, PD-2.5, PL-2.5, threaded pin	800 rpm, 25 mm/min, 3º	Al powder - 50 µm, Al_2O_3 - 50 nm, Air Plasma Spraying	1	Homogeneous dispersion of RPs, Increase in hardness, Improvement in wear properties[41].
AA6063 (200L, 60W, 4.75T)	H13 steel tool, SD-20, PD-6, PL-3, threaded pin (M6 × 1), tool offset from 0 to 2 mm in steps of 0.5mm.	1120 rpm, 40 mm/min, 2.5º, tool plunge depth - 0.25 mm	SiC, 10 µm, Direct Pasting, Groove (2×2 mm^2) and Blind Holes	1	Groove technique is found better as compared to direct pasting and blind holes techniques. Tool center offset towards the retreating side produces defect-free SCs. 1.5 mm offset which is half the radius of the tool pin gives the optimum value[42].
AA6061 (200L, 60W, 5T)	H13 tool steel, SD-20, PD-6, PL-2.5, threaded pin	1400 rpm, 40 mm/min, 2.5º, tool plunge depth varying from 0.10 mm to 0.35 mm in steps of 0.05 Mm	SiC, 10 µm, Groove (2×2 mm^2)	1	The particle dispersion in the matrix was found better with an optimum TPD of 0.25 mm. Above this value of optimum TPD (0.25), various problems occur such as sticking of work piece to the shoulder, flashing of RPs, and damage to the specimen[43].

(*Contd.*)

Table 1—Summary of various features of FSP: dimensions of specimen used, tool material, tool geometry, process parameters and techniques used in fabrication of aluminium alloy and its composites.

(SD: Shoulder Diameter; PD: Pin Diameter; PL: Pin Length; AF: Axial Force, TPD: Tool Plunge Depth; EDM: Electric Discharge Machine) — (*Contd.*)

Material of the specimen and its size in mm (L-Length, W-Width, T-Thickness	Tool material and its geometry (All dimensions are in mm)	FSP operational parameters (rotational speed, traverse speed, tool tilt angle, axial force)	Reinforcement type, its size and techniques (groove dimension: width × depth)	No. of Passes	Prominent Remarks
Al7075 (150L, 50W, 6T)	D2 Steel, SD-18, SL-25, PD-6, PL-5.5, con-cave shoulder, threaded pin	600 rpm, 20 mm/min, 1º, AF- 10 KN	SiC, 3.6 µm and Carbon Black (CB, Grade-P842)	1	Increase in grain refinement, microhardness, ultimate tensile strength (by 2.5 times), ductility, and reduction in wear rate are observed[44].
Al5083 (150L, 80W, 6T)	FSP tool with pin and without pin	1600 rpm, 20 mm/min	SiC- 5 to 20 µm, Carbon Nano Tubes (CNTs) - 5 to 20 nm in outer diameter, 1-10 µm in length, Groove - (1× 2.5 mm2)	3	Uniform distribution of RPs, significant grain refinement, increase in hardness (1.35 to 1.5), and enhancement in tensile strength are noted[45].
Al1050 (84L, 50W, 3T)	SD-12, PD-3, PL-2.1	1200 rpm, 50 mm/min, 3º	SiC, 50 nm, Groove (1 × 1.5 mm 2 and 2 × 1.5 mm2)	3	Increase in yield strength and Orowan strengthening was found with SiC as RP[46].
AA1060 (200L, 200W, 4T)	Single pin tool and multi-pin tool	800,900,1300 rpm;40,60,80 mm/min; plunge depth- 0.2, plunge pressure-13 MPa	SiC, 40 µm, Blind Holes (3 mm diameter, depth- 5 mm, 5 mm space between holes)	1	Improvement in refinement and better distribution of SiC particles with multi-pin tool results in an enhancement in microhardness and reduction in wear loss. An increase in friction and plastic deformation was also found with multiple pins[47].
Pure Al (150L, 50W, 6T)	D2 Steel, SD-18, SL- 25, PD-6, PL-5.5, con-cave shoulder, threaded pin	600 rpm, 20 mm/min, 1º, AF-10 KN.	Bare SiC, SiC coated with Al2O3 and SiC coated with ZnAl2O4	1	Better grain refinement and microhardness (2 times) was observed with SiC particles[48].
Al3003 (100L, 50W, 5T)	SD-18, PD-3, PL-4.3	1200 rpm, 50 mm/min, AF- 10 KN	TiO2, Groove, reinforcement weight % - 0 to 6 % with an increment of 1.5	1	The size of grain was reduced by 70%. RPs in composite enhanced the tensile strength and microhardness (highest microhardness was found with 6% weight fraction ofTiO2) [49].
Al-Zn-Mg alloy AA7075 (200L, 70W, 20T)	X210Cr12, SD-25, Cone pin (Diameter at shoulder - 5mm, Diameter at tip – 3.6 mm, PL- 3.8)	400,600 rpm , 50 mm/min, 3º	B4C, 20 µm, Groove (1 × 2 mm2)	4	Better distribution of RPs with increase in FSP passes. Enhancement of microhardness and wear resistant properties. Work piece developed at 600 rpm with 4 FSP passes produced the highest hardness[50].

(*Contd.*)

Table 1—Summary of various features of FSP: dimensions of specimen used, tool material, tool geometry, process parameters and techniques used in fabrication of aluminium alloy and its composites.

(SD: Shoulder Diameter; PD: Pin Diameter; PL: Pin Length; AF: Axial Force, TPD: Tool Plunge Depth; EDM: Electric Discharge Machine) — (*Contd.*)

Material of the specimen and its size in mm (L-Length, W-Width, T-Thickness	Tool material and its geometry (All dimensions are in mm)	FSP operational parameters (rotational speed, traverse speed, tool tilt angle, axial force)	Reinforcement type, its size and techniques (groove dimension: width × depth)	No. of Passes	Prominent Remarks
AA5083- H112 Alalloy (100L, 60W, 5T)	H13 steel tool, SD-15, PD-4.5, PL-3.5	1400 rpm with 60 mm/min, 2.5º, tool plunge depth - 0.2 mm.	WC, 4 µm, Groove (2 × 3 mm2)	4	Grain size decreased, higher hardness, and better wear resistance are observed[51].
AA1050 (200L, 160W, 3T)	H13 tool steel	1200,1600rpm; 100, 200, 300mm/min.	TiC, 60 µm, V-Groove of about 5 mm	1	RPs distributed uniformly with tool rotational speed of 1200 rpm and traversal speed of 100 mm/min resulting in improvement in hardness and wear resistant properties[52].
AA6061 (100L, 50W, 8T)	HCHCr Steel, SD-18, PD-6, PL-5.7, hexagonal pin profile	1200 rpm, 50 mm/min	Al3Zr, 0 to 15 weight % with an increment of 5	2	Homogeneous distributions of RPs, elimination of casting defect, refinement of grains, and improvement in tensile strength are obtained[53].
AA6061 (100L, 50W, 8T)	HCHCr Steel, SD-18, PD-6, PL-5.7, hexagonal pin profile	1200 rpm, 50 mm/min	Al2Cu, 0 to 15 weight % with an increment of 5	2	FSP resulted in homogeneous distribution of particles, broke down of large Al2Cu particles into fine sized particles, and improved elimination of casting defect pores, grain refinement, and tensile strength[54].
AA1050 (200L, 60W, 10T)	HCS tool, SD-18, PD-6, PL-5	1400 rpm, 40 mm/min, plunge depth - 0.2 mm	Ni - 20 µm, Ti - 40-60 µm, C - 50µm, Blind Holes (2 mm diameter and 3 mm depth with space of 1 mm)	2, 4 and 6	Enhancement of homogeneous dispersion of RPs in aluminum matrix with 6 FSP passes resulted in uniform distribution of RPs and increase in tensile strength and microhardness[55].
Al7075 (6.35T)	FSP tool, SD-10, PD-4, PL-2.2, threaded pin	1500-2500 rpm, 2.5 mm/s, plunge depth- 0.03 – 0.24mm	Multi-Walled Carbon Nano Tubes (MWCNTs), covering of Groove (0.3 × 2.3 mm2) by thin sheet (Al 6111, 1.1 mm thick)	1	Improvement in the distribution of nanotubes by increasing the rotational speed and plunge depth are obtained[56].

3.2 Size and volume % of reinforcement particles

The fractional volume of RPs used defines the strength of composite material. The percentage of the volume fraction is adjusted by changing the groove size as shown in Fig. 5, Equations 1 and 2.

$$Theoretical\ volume\ fraction = \frac{Groove\ area}{Tool\ pin\ projected\ area} \times 100 \quad \ldots (1)$$

$$Actual\ volume\ fraction = \frac{Groove\ area}{Surface\ composite\ area} \times 100 \quad \ldots (2)$$

where, groove area is equal to product of the depth of groove and width of groove; tool pin projected area is equal to the pin diameter and pin length

It is found from literature that the nano-sized RPs exhibit better micro structural as well as mechanical

properties as compare to micronized RPs. The grain size was estimated by Zener's formula (Eq. (3))[58]:

$$\overline{R} = {}^{4r}/_{3f} \quad \ldots (3)$$

Where, $\overline{R}$ is the average radius of curvature of the grain boundaries, r the radius of the particles of the second phase and f is the volume-fraction of particles.

Inter-particle spacing (λ) between adjacent particles is calculated by (Eq.(4))[59]:

$$\lambda = \frac{(1-V_p)}{N_L} \quad \ldots (4)$$

where, V_p is the particle's volume fraction, N_L is the number of particle intercepts per unit length.

3.3 Strategies of reinforcement

Broad classification of reinforcement strategies incorporating FSP are shown in Fig. 6.

The direct pasting technique of reinforcement was initially used by Mishra *et al.*[60]. Some volatile solvent mixed with RPs are directly pasted over the base plate[61,62]. Plasma spray[63] and high velocity oxy fuel (HVOF)[40,41] techniques are also used for direct pasting. In this technique, the ejection of the RPs is the major problem. Recently, the most popular technique used for creation of MMC surfaces is the groove technique[37,39,40,44,47–50,56,65]. The schematic operational view of SC fabrication using the groove technique is shown in Fig. 6. In this technique first, a groove is made. Wire EDM is mostly used for making this groove. Then a packing of RPs is inserted into the groove, then the FSP tool without pin is operated on that groove to avoid the ejection of RPs during processing. Finally, FSP with a pin is performed along the specified path. In some studies[56], this groove is covered by a thin sheet (Fig. 7 (a)). Blind

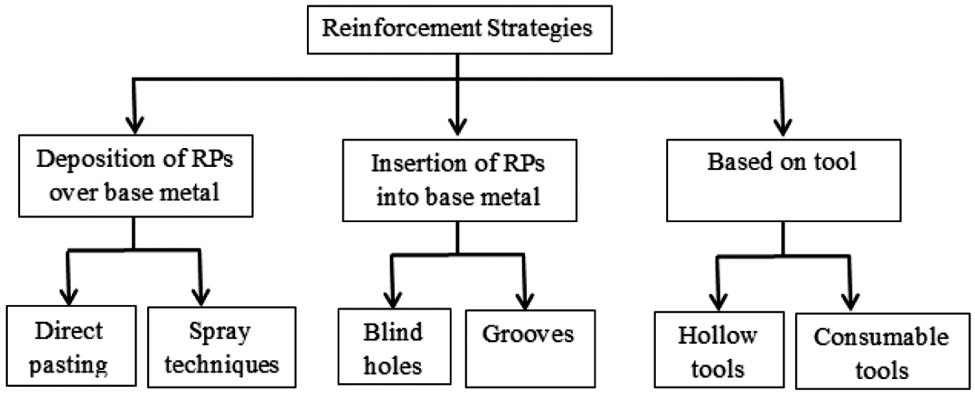

Fig. 5 —Operational view of FSP (a) Machining of groove, (b) Inserting of RPs into groove, (c) Closing of groove with pin-less FSP tool and (d) FSP with tool having pin.

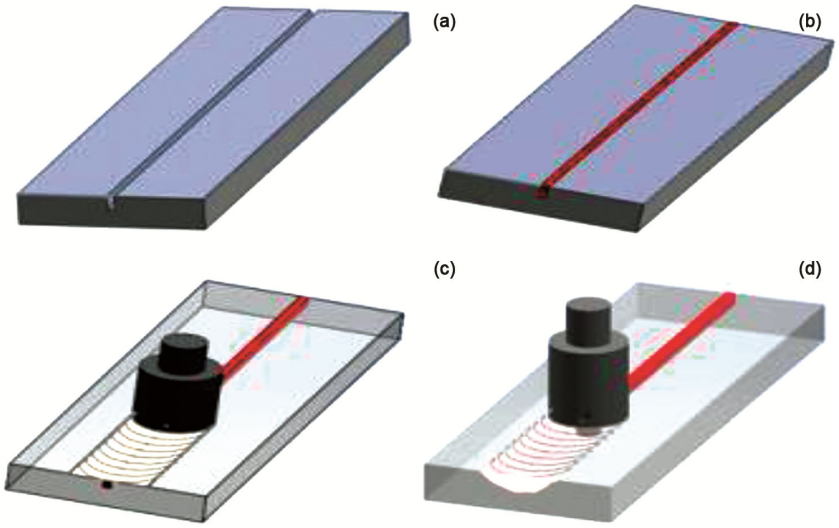

Fig. 6 — Classification of reinforcement strategies[64].

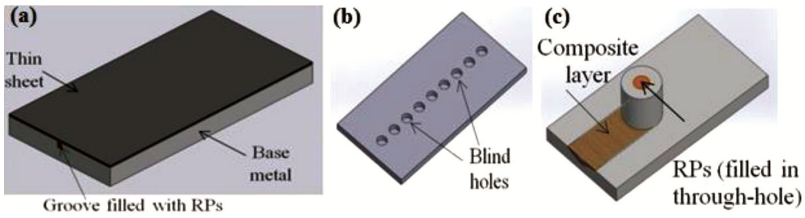

Fig.7 — (a) Schematic representation of covering of groove by thin plate, (b) Reinforcement method through blind drilled holes and (c) Direct friction stir processing (DFSP) method.

drilled holes are another method to reinforce particles into the base metal (Fig. 7. (b))[38,45,53].

In this technique, during processing, half part of the shoulder ahead of the tool pin covers the opening of the holes. Also, an alternative method of Direct Friction Stir Processing (DFSP) is used by Huang *et al.*[66] (Fig. 7 (c)).

4 Influence of RPs

The reinforcement particles used should be compatible with the base metal. The reinforcement type, its size, and fractional volume depend on the end-use application of the product. The effect of various RPs is summarized below:

Al_2O_3: Increase in wear resistance is observed with an increase in rotational speed. Surface composites fabricated in high heat input condition results in higher hardness and defect-free stir zone[38]. By increasing the volume % (2%, 4%, and 6%), micro hardness increases while yield stress, UTS, and % of elongation decrease[39]. Homogeneous distribution of RPs, increase wear resistance, hardness, and strength[40,41].

Some of the other reinforcement particles are:

SiC: Significant grain refinement, increase in mechanical properties and reduction in wear loss are observed[42–48].

TiO_2: Grain size reduction, enhancement of hardness and tensile strength, hardness is maximum with 6% TiO_2[49].

B_4C: Enhancement of hardness and wear resistance are observed[50].

WC: Grain size reduction, higher hardness and better wear resistance are obtained[51].

TiC: Improvement in hardness, wear resistance and strength of the processed specimen are noted[52].

Al_3Zr: Refinement of grains, improvement in tensile strength, and elimination of casting defect pores is achieved[53].

Al_2Cu: Homogeneous distribution, elimination of casting defect, grain refinement, and tensile strength improvement are found[54].

Combined effect of Ni, Ti, and C: Better dispersion of RPs in Al matrix with six FSP passes, uniform distribution of RPs resulted in increase in micro hardness and ultimate tensile strength[55].

MWCNTs: Multi-Walled Carbon Nano tubes allow higher rotational speed and plunge depth and multiple FSP passes improve the uniform distribution of nanotubes[56].

5 Microstructure and Mechanical Properties of Processed Specimen

The influence of refinement of microstructure and mechanical properties like strength, hardness with different process parameters, reinforcement type, its size, and fractional volume %, strategies of reinforcement are mentioned in Table 1. With more number of FSP passes and by altering the direction of the rotating tool, agglomeration of particles was eliminated, homogeneous distribution of RP achieved, reduction of grain size and enhancement of micro hardness, tensile strength and wear resistance are obtained[37,38,45,46,50,51,55]. The most commonly used material for FSP tool is H13 tool steel[37,38,40,42,43,51,52,56,65,66]. D2 steel, HCS, HCHCr, X210Cr12 steels are also used by some researchers[44,48,50,53–55]. For SiC RPs, tool rotational speed of 1150 rpm to 1400 rpm with tool travel speed of 20 mm/min to 60 mm/min is mostly used. But in case of Al_2O_3, travel speed up to 100 mm/min is usually selected. Axial forces of 5 KN to 10 KN are applied in practice[39,44,48,49]. Plunge depths of 0.15 to 0.35 mm are reported by few scientists[40,42,47,51,55,56]. Some authors reported tool tilt angle of 1º, 2.5º and 3º [37–40,42–44,46,48,56]. With tool tilt angle, homogeneous distribution of RPs, reduction in grain size is found. Enhancements of grain refinement resulted in better strength, higher hardness, and better wear resistance. Groove technique was found to be better and mostly used technique as compared to other reinforcement techniques like direct pasting, blind holes and DFSP[37,39,42,43,45,46,49–51,64]. Few studies of direct pasting by spray techniques of RPs are also reported in the

literature[40,56]. As in all these techniques chances of sputtering of particles is more, so wastage of RPs is observed. A low cost FSP machine was designed and microstructure refinement and mechanical properties are studied by Hans Raj *et al.*[67].

6 Coefficient of Friction (COF) and Wear Characteristics

Microstructure and mechanical properties like tensile strength, micro hardness, ductility, etc. of Friction Stir Processed (FSPed) specimen are discussed extensively by various authors, however, only a few studies on COF, Wear, Fatigue, Corrosion, and Tool wear are reported. The summary of investigation of tribological tests is presented in Table 2. It is observed from experimental studies of COF versus sliding period that the value of friction coefficient increased at the beginning stage and then reduced and became steady after some time[35,38,51,68–71]. In few studies, the average COF increases with increase of load[72–74]. In a study[75], its value first decreases and then increased with increase of load. The average COF decreases considerably by increasing the number of FSP passes[35,70,71]. In the study of Yuvaraj *et al.*[71] the average COF with 3-passes is lesser as compared to single pass processed specimen. Barenji *et al.*[70] reported the average COF for processed specimen with two and four passes are 0.41 and 0.29 respectively, which is much lower than the average COF of 0.68 of base metal. Furthermore, Mazaheri *et al.*[76] observed that the friction coefficient initially increased with 2-passes and then decreased with 3-

Table 2— Summary of the investigation of Coefficient of Friction (COF) and Wear behavior.

Samples prepared for Tribological test (as-received specimen and reinforced specimen)	Tools and Apparatus Used	Tribological testing Parameters	Prominent Remark / Finding
Al 6061/SiCFSPed with 1-pass, 2-pass, 4-pass, AL6061/SiCFSPed with different pin profile (Smooth, Square, Threaded, Triangle)	Pin-on-disc tribometer, Scanning Electron Microscopy (SEM)	Normal load - 40 N, sliding velocity - 0.35 m/s	The wear resistance is improved by increasing the number of FSP passes. With more FSP passes, uniform distribution of SiC particles and finer grains are obtained resulting in decreased wear rate. The square pin and straight cylindrical pin exhibited higher and lower wear resistance respectively[35].
AA5083 and AA5083/AL_2O_3 (Base alloys, Low Heat (LH) condition base alloy, High Heat (HH) condition base alloy, LH condition composite, HH condition composite.)	Ball-on disc tribometer, Profilometer, Scanning Electron Microscopy with Energy Dispersive X-Ray Spectroscopy (SEM-EDS)	Rotational speed of ball - 500 rpm, linear speed - 0.0785 m/s, total duration - 25 min, total sliding distance - 117.75 m , normal load applied - 5, 10 and 20 N	Wear rate increases gradually on increasing the normal load applied[38].
AA7075, AA7075/SiC, AA7075/SiC/Carbon Black (CB)	Pin-on-disk tribometer, XRD, Field Emission-SEM (FE-SEM)	Sliding velocity - 2, 4, 6 m/s, sliding distance - 1000, 1500, 2000 m, normal load - 49.03 N	Total 81 numbers of experiments were conducted using Taguchi Orthogonal Array Design to observe the wear behaviour before and after FSP. It was observed that addition of SiC and CB significantly reduces the wear rate[44].
Al7075 and AA7075 + B_4C (FSPed samples without reinforcement - M4-400 and M4-600 (4 passes, 400 rpm and 600 rpm), FSPed Samples F4-400, F4-600, C4-400, C4-600 (F - stands for flat pin less tool and C - for the cone shape pin tool, 4 passes, 400 rpm and 600 rpm.)	Flat-on-cylinder tribometer, Stylus profilometry, 3D digital microscopy, SEM-EDS, bending load cells and a linear variable differential transducer.	Normal applied load - 5 N, Linear speed - 0.3 mm/sec, total sliding distance - 1000 m	Improvement in wear resistance and COF with addition of B_4C particles as compared to unreinforced FSPed material is recorded[50].
AA5083, FSPed AA5083, Al-WC Additive friction stir processing (AFSP) surface composite	ball-on-disk tribometer, SEM-EDS, XRD	Sliding velocity - 10 mm/s, sliding time - 15 min, normal load - 2.3 N.	The COF of AFSP surface composite was lower as compared to as-cast Al alloy[51].

(*Contd.*)

Table 2— Summary of the investigation of Coefficient of Friction (COF) and Wear behavior.— (*Contd.*)

Samples prepared for Tribological test (as-received specimen and reinforced specimen)	Tools and Apparatus Used	Tribological testing Parameters	Prominent Remark / Finding
Al7075 FSPed, Taguchi L27 design of experiments conducted with FSP parameters (Tool rotational speed - 800, 1150, 1500 rpm, Traverse speed - 20, 40, 60 mm/min, Number of passes - 2, 4, 6)	Pin-on-disc wear testing machine, SEM	Normal load - 19.62 N, sliding velocity - 2 m/s, sliding distance - 2000 m	The wear rate decreases with higher traverse speed. A decreasing trend of wear is noticed for the entire specimen processed up to 4-passes. The specimen processed with 1150 rpm showed the minimum wear as compared to that specimen processed at 800 rpm and 1500 rpm. The lowest average COF was reported for the specimen processed with 4-passes at 1150 rpm and 60 mm/min[68].
Al/ 12 weight % Si alloy	Pin on disc tribometer, Optical microscope	Sliding distance - 100 m, total duration - 16 min, normal loads applied - 2.5N, 5N, 7.5N, 10N, sliding speed - 0.1 m/s.	There was no significant change found in the average COF of as-cast samples and FSPed samples. The weight loss increased almost linearly with increasing applied normal load for both the samples. The weight loss for FSPed samples is significantly lower as compared the as-cast sample[69].
Al6061 and Al6061-Al2O3/TiB2 surface hybrid composites (SHC) with 1-pass, 2-pass and 4-pass FSP	Pin-on-disc tribometer, SEM	Sliding velocity - 0.5 m/s, total duration - 2000 s, normal load - 50 N.	The average COF is higher in base metal and gets decreased with increasing of number of passes. The lowest COF was found with 4-pass SHC FSPed specimen[70].
Al5083, Al 5083 FSPed with 1-pass, Al5083-B4C (micro and nano size particle) FSPed with 1-pass and 3-pass	Pin-on-disc tribometer, SEM	Sliding velocity - 2 m/s, normal load - 30 N, sliding distance - 3000m	The weight loss of nano particle FSPed specimen is lowest as compared to other specimen. 3-pass nano particle FSPed specimen showed the lowest weight loss. The nano particles of reinforcement and more number of passes results in better wear properties[71].
AA 8011, AA 8011 with Shape Memory Alloy (SMA), AA 8011/(SMA + Si3N4)	Pin-on-disc tribometer, SEM	Normal load - 10, 20, 30, 40 N, sliding distance - 1000 m and 2000 m, sliding speed - 0.22 m/s and 0.44 m/s	The wear rate of the processed samples goes higher as the load and sliding distance is increased. The wear resistance is 53 % more with hybrid composite and 26% more with AA 8011 with SMA as compared to AA8011 base alloy. The COF decreased as the load and sliding distance increased[72].
Al 1120, Al/Graphite, Al/MoS2	Pin-on-disc tribometer, SEM	Sliding velocity - 2.62 m/s, sliding distance - 3000 m, load applied - 15, 20, 25, 30, 35 N	Wear loss is lower with the graphite reinforced SC as compared to MoS2 reinforced composite and base metal. Moreover, weight loss increased by increasing the sliding speed in all the samples. Weight loss also increased with increase of load applied. The lowest wear rate was found in the graphite reinforced specimen with15 N load. The COF increased on increasing the load. The COF of the Al/Graphite SC was less as compared to that of Al/MoS2[73].

(*Contd.*)

Table 2— Summary of the investigation of Coefficient of Friction (COF) and Wear behavior.— (*Contd.*)

Samples prepared for Tribological test (as-received specimen and reinforced specimen)	Tools and Apparatus Used	Tribological testing Parameters	Prominent Remark / Finding
Al5083, Al without particle, Al/TiC, Al/B_4C, AL/(TiC+B_4C) hybrid composite	Ball-on-disk tribometer, SEM-EDS	Sliding distance - 3000 m, normal load applied - 20 to 100 N with increment of 20 N.	Wear resistance is remarkably improved with addition of the RPs in all sliding loads. The lowest wear rate is observed with hybrid composites as compared to all samples[74].
Al 1050/(Al_2O_3+SiC), different hybrid ratio of reinforcements - 10% to 100% in the step of 10%	Ball-on-disk tester, SEM	Sliding velocity - 31.4 mm/s, normal loads - 2, 5 N	The average COF value decreases with increase in the Al_20_3 content ratio. Moreover, the average COF decreases with increase in the load applied from 2 N to 5 N. Addition of RPs was beneficial in reducing the wear volume losses[75].
Al6061 with 2-pass, 3-pass and 5-pass FSPed composite and Al6061/SiO_2 with 2-pass, 3-pass and 5-pass FSPed composite	Pin and disk tribometer, SEM-EDS, x-ray diffraction (XRD)	Sliding speed - 0.1 mm/s, normal force - 20N, sliding speed - 1000 m	Weight loss increases gradually by increasing the sliding distance for both cases (FSPed with and without reinforcement). Weight loss trend of 2-pass FSPed in both cases is higher as compared to the samples processed at other FSP passes. Increasing the number of FSP passes results in decrease in both COF and weight loss[76].
AL5083/(Al_2O_3+graphite powder), Graphite Hybrid Ratio (Gr.H.R. in %): 20, 40, 60, 80, 100 %	Pin-on-disc tribometer, SEM	Sliding speed - 0.24 m/s, sliding distance - 950 m, normal load - 24.8 N.	Wear rate of nano-composites decreases on increasing the Gr.H.R. Wear rate was found lowest with Gr.H.R. of 75%. COF is also affected by Gr.H.R. Average COF decreases continuously as Gr.H.R increases[77].
AA6082/(Y_2O_3 + Graphite)	Pin-on-disk wear tester	Normal loads applied - 20, 40, 60 N, sliding speed - 1 m/s, sliding distance - 2000 m	Composites contain 8% volume fraction of Graphite and 2% volume fraction of Y_2O_3 exhibited minimum wear rate. Wear rate increased by increasing the applied load. The value of COF is found to be lowest with 7 %. After addition of more graphite beyond the 7%, it starts increasing[78].
Al 7075 and FSPed AA7075/(SiC+Graphite)	Pin-on-disc tribometer, SEM	Sliding distance - 1400 meters, normal load - 10 N, sliding velocity - 4 m/s	The values of wear rate and COF of processed specimen are lower as compared to those of base metal[79].
Al 6082/ZrO_2 (Base material, 0% ZrO_2FSPed, 5% ZrO_2FSPed, 10% ZrO_2FSPed, 15% ZrO_2FSPed)	Pin on disc tribometer, SEM	sliding speed - 1 m/s, normal load - 40 N, sliding distance - 3000 m.	FSPed sample with 15% volume fraction exhibited maximum wear resistance. The wear rate and the average COF decreased with increase in volume fraction of RPs[80].
Al6061, AL/TiB_2 (volume percentage of particles - 2, 4, 8 %)	Pin-on-disk tribometer, SEM	sliding speed - 3.4 m/s, normal load - 40 N.	Wear rate decreases as the volume percentage of TiB_2 increases[81].
AA6082, AA6082/TiB_2, AA6082/(TiB_2 + BN), AA6082/BN	Pin-on-disc tribometer, SEM	Sliding velocity - 1m/s, normal force - 20 N, sliding distance - 2500 m.	The incorporation of both TiB_2 and BN as a RPs reduced the wear rate of composites. The lowest wear rate is found in AA6082/(TiB_2 + BN) hybrid composites as compared to both the mono composites AA6082/TiB2 and AA6082 /BN[82].

(*Contd.*)

Table 2— Summary of the investigation of Coefficient of Friction (COF) and Wear behavior.— (*Contd.*)

Samples prepared for Tribological test (as-received specimen and reinforced specimen)	Tools and Apparatus Used	Tribological testing Parameters	Prominent Remark / Finding
AA6063/SiC	Ball-on-disk tribometer	Normal load - 30, 40, 50 N, sliding speed - 500 rpm, sliding distance - 500 m, 1000 m, 1500 m, SiC weight % - 0.5, 1, 1.5 %	The sliding distance has the largest contribution on wear loss. The COF is mainly affected by the weight % of SiC as compared to other process parameters[83].
Al 7075 substrate withour FSP, Al7075/SiC with constant tool speed of 710 rpm and different traverse speed 20, 40, 56 mm/min	Wear test apparatus	Sliding speed - 2.5 cm/s, normal load - 2, 4, 5N	The wear rate and average COF increased with an increase in load. At a constant load of 2N, the specimen processed with 710 rpm and 56 mm/min exhibited lower wear rate. The wear and friction characteristics improved with addition of RPs[84].
AA1050 and AA1050-TiC	Pin-on-disc tribometer, SEM	Sliding distance - 2000 m, normal load applied - 25N	Investigated the effect of processing parameters on the wear behaviour of FSPed Al-TiC composites. The optimum combination of these parameters improved the wear resistance[85].
Cast, FSP-AGG, FSP-fine (Cast: as cast A356 subjected to T6 heat treatment (HT), FSP-AGG: HT of FSPed specimen with 1500 rpm and 102 mm/min of tool rotational speed and traverse speed respectively, FSP-fine: HT of FSPed specimen with 300 rpm and 102 mm/min)	Electron back-scattered diffraction (EBSD)	Not mentioned	Crack initiation occurred mostly in the Cast samples at microstructural defects such as porosities, inclusions. FSP-AGG and FSP-fine conditions exhibited very large improvements in life up to 10 times as compared to the cast sample[86].

passes and subsequently slight enhancement of COF is found with 5-passes. The size of RPs also affected the friction coefficient. The lower value of average coefficient is found with nano-sized RPs as compared to base metal[71]. Moreover, the average COF is affected by the volume % of reinforcement used in the hybrid composites. The higher content ratio of Al_2O_3 in the hybrid ratio of Al_2O_3/SiC reduces the average COF[75]. The higher volume fraction of graphite in the hybrid ratio decreases the COF[77,78].The value of COF is found to be lowest in case of hybrid composites as compared to mono composites and base metal[72,74,79].

In literature most of the authors investigated wear values in terms of volume wear rate and mass wear rate. Vijayavel *et al.*[87] studied the wear behavior by varying the pin volume ratio and found that the specimen fabricated by tapered cylindrical pin has lowest COF and lowest wear rate as compared to other pin profiles. In the review paper of Ikumapayi *et al.*[88], a brief description of wear behavior of various non-ferrous alloys along with aluminum alloy is discussed. In literature, it is reported that the wear loss reduced with an increase in the number of FSP passes. Girish *et al.*[68] reported that wear rate in FS Preduced up to 4-passes and increased after 5th pass for almost every combination of rotational and traverse speed. Mazaheri *et al.*[76] found that the weight loss is lowest in processed sample with 5-pass composite as compare to 1-pass, 2-pass, and 3-pass processed samples. Eftekharinia *et al.*[35], observed reduction in wear rate trend by increasing the FSP passes at all sliding conditions. Barenji *et al.*[70] reported that the weight loss decreases as the number of FSP pass increases. Wear resistance was significantly improved in surface hybrid composites after 4-passes of FSP as compared to 2-passes and a single pass FSP. Yuvaraj *et al.*[71] observed that use of the nano-sized particles exhibited lower wear rate as compared to micro-sized reinforced particles.

Reinforcement played a vital role in wear. The addition of reinforcement reduces the wear loss[50]. Roy *et al.*[44] concluded that the addition of reinforcement increases the wear resistance. Yuva raj *et al.*[80] also found that the wear resistance increased as volume fraction of reinforcement increased. Wear rate is highest for 15% volume fraction of reinforced particles as compared to 0%, 5%, 10%. Kishan *et al.*[81]

also reported that on increasing the volume percentage of reinforcement, the wear rate decreased. In the review paper of Gupta *et al.*[89], effect of various reinforcements on wear is presented. Velickovic *et al.*[90] studied the tribological properties of nano-composites and concluded that the nano-sized RPs generally exhibited higher wear resistance and lower COF. Various authors reported that the hybrid composites have better wear resistance as compared to mono composites[70,72,74,91–93]. Dinaharan *et al.*[94] used the fly ash particles and aluminum as a base metal and found improvement in the wear resistance of the composite. The wear loss decreases as the volume fraction of fly ash particles increases. The graphite reinforced composites exhibited better wear reduction as compared to other reinforcement materials such as molybdenum[73] and Al_2O_3[75].

The wear rate is affected by the sliding distance[35,68]. The wear rate trend of composite material is constant with respect to sliding distance[73,80,81]. The weight loss trend increased with increase in sliding distance for every specimen processed with different FSP passes[70,71,73,76]. Rajesh *et al.*[83] reported that the sliding distance contributes a major role to minimize the wear rate.

In most of the studies, it is observed that the higher wear is associated with the increase in normal load[38, 72–75,78,84,95]. Aktarer *et al.*[69] conducted the experiments and found that the weight loss versus normal load exhibited almost a linear curve for both FSPed samples and as-cast base sample.

Sathiskumar *et al.*[96] reported the effect of the rotational speed of the tool. The size of the wear debris and the wear rate increased as the tool rotational speed increased. Akinlabi *et al.*[85] investigated the effects of processing parameters on the wear behavior. The rotational speed and the feed rate are analyzed and models are developed by them to predict the wear behavior. Yadav *et al.* [38] analyzed the wear rate of specimens processed at high heat input condition with 1400 rpm and 40 mm/min and low heat condition with 710 rpm and 100 mm/min. They concluded that the wear rate is lowest in high heat condition for various loads (5N, 10N, and 20N) as compared to specimen processed with low heat condition. Defect free stir zone is obtained in the specimen processed in high heat condition.

7 Fracture and Fatigue behavior

Aluminum alloys are widely used in various industries especially in automobile industry. Various engine parts are made up of aluminum alloys. Few parts are subjected to fluctuation of temperature and cyclic loading which causes fatigue failure[97]. A356 aluminum alloy is mostly used because of its high strength, wear resistance, good cast-ability, but has poor fatigue performance[98]. This poor fatigue performance is mainly because of the microstructural defects such as porosity, inclusion, agglomeration of particles[99–105]. Sharma *et al.*[106] investigated the effect of FSP on fatigue behavior of A356 aluminum alloy and concluded that the FSP can be used to modify the microstructure in regions undergoing high fatigue loading and thus improve the overall performance of base metal. Hussein *et al.*[107] analyzed the fatigue and fracture behaviors of AA5083-H111 aluminum alloy using Scanning Electron Microscopy (SEM) and found better fatigue properties in FSPed sample as compared to base metal and the specimen fabricated through friction stir welding. Nelaturu *et al.*[86] studied the effects of microstructures on the fatigue mechanisms of crack initiation and crack propagation and concluded that the crack initiation occurred in that particular area of cast samples which was affected by micro structural defects. They also concluded that the life of FSPed specimen is improved up-to 10 times as compared to the base metal. Sun *et al.*[108] also concluded that the fatigue performance is better in aluminum alloy A206 FSPed specimen as compared to as-cast specimen A206. The increased performance under fatigue is responsible for enhancement of strength and reduction of the crack nucleation sites. Roy *et al.*[44] observed the fracture behavior of Al 7075 alloy with the help of field emission scanning electron microscope for the specimens before and after FSP and with and without reinforcements.

8 Conclusions and future scope

FSP is a solid phase processing, versatile, and eco-friendly technique, without any adverse effects. Al alloy is light in weight but after incorporating RPs using FSP, it exhibits enhancement of mechanical properties like increase in strength and increase in hardness. Metal matrix composites are useful in industries like automobile, aerospace, marine, construction work, etc. FSP is now applied frequently in preparation of surface MMCs, microstructure improvement of casting materials, softening and plasticizing the processed materials. In this article, a review is attempted based on various FSP parameters, reinforcement variables, and strategies of reinforcement. Consolidated results of various researchers depicting the effect of various parameters of FSP and use of reinforced particles on microstructure, hardness, strength of processed composites is illustrated with the help of Table 1. The groove technique is mostly used by various authors for

preparing MMCs and found to be better than other reinforcement techniques. It is reported in the literature that multi pass FSP are an efficient way to achieve uniform dispersion of reinforcement particles (RPs) in the MMC. Tool offset may be one of the techniques to get uniform distribution of RPs in a single pass FSP. The tool pin profile plays a vital role in FSP. For achieving adequate mixing of RPs with base metal in minimal FSP passes, an optimum pin profile is required. The threaded pin is more efficient in case of nonferrous alloys specially Al alloys, while in case of hard metals like stainless steel, threaded pin causes excessive wear of tool which increases the cost of production. The rotation of tool direction in successive FSP passes is responsible for the homogeneous dispersion of RPs. The higher ratio of tool rotation speed to traverse speed and number of passes generates more heat resulting in finer grain formation, enhancement in strength and hardness.

The friction coefficient and wear characteristics of processed specimen with or without reinforcement are presented in Table 2. The value of COF and wear are influenced by the number of FSP passes, normal load applied, size and volume fraction of reinforcement, hybrid composites, pin profile, combination of rotational and traverse speed. The average COF and wear is not much affected by the sliding distance. The number of FSP passes significantly affected the COF and wear. Its value decreases with increasing the number of passes. After five passes wear rate starts increasing. Most of the researchers concluded that the addition of reinforcement reduces the wear rate. Nano-sized reinforcement and hybrid composites have exhibited better wear resistance and lower COF. The addition of more graphite improved the wear properties. FSP is gaining recognition and is now extended to the fabrication of polymer matrix composites, metallic foams, porous materials, multifunctional metals like piezoelectric ceramic composites, magnetic ceramic composites, etc.

Acknowledgements

The authors acknowledge Most Revered Professor Prem Saran Satsangi Sahab, Chairman, Advisory Committee of Dayalbagh Educational Institutions for his inspiration and motivation.

References

1 Annigeri U K & Veeresh Kumar G B, *Mater Today Proc,* 4 (2017) 1140.

2 Sevinç Adiloğlu, I, Chaochao Yu, Rui Chen, Juan Jinxing Li, Juan Jinxing Li, Martin Drahansky, M.t Paridah, Amin Moradbak, A.Z Mohamed, Hongqhan abdulwahab taiwo Owolabi, FolaLi, Mustapha Asniza, Shawkataly H.P Abdul Khalid, Taruna Sharma, Neeraj Dohare, Meena Kumari, Upendra Kumar Singh, Abbul Bashar Khan, Mahendra S Borse, Rajan Patel, Angela Paez, Anna Howe, Degussa Goldschmidt, Chemical Corporation, John Coates, *Intechi,* (2012) 13.

3 Sharma A K, Bhandari R, Aherwar A & Pinca-Bretotean C, *Mater Today Proc,* 27 (2019) 1608.

4 Shi J L, Yan H G, Su B, Chen J H, Zhu S Q & Chen G, *Mater Manuf Process,* 26 (2011) 1236.

5 Srivatsan T S & Lavernia E J, *J Mater Sci,* 27 (1992) 5965.

6 White J & Willis T C, *Mater Des,* 10 (1989) 121.

7 Mahmood M A, Popescu A C & Mihailescu I N, *Materials (Basel),* 13 (2020).

8 Marimuthu S, Dunleavey J & Smith B, *Procedia CIRP,* 85 (2020) 240.

9 Halil K, Ismail O I, Sibel D & Ramazan Çi, *J Mater Res Technol,* 8 (2019) 5348.

10 Manohar G, Dey A, Pandey K M & Maity S R, *AIP Conf Proc, 1952* (2018).

11 Bodukuri A K, Eswaraiah K, Rajendar K & Sampath V, *Perspect Sci,* 8 (2016) 428.

12 Yun E, Lee K & Lee S, *Surf Coatings Technol,* 191 (2005) 83.

13 Lee J, Euh K, Oh J C & Lee S, *Mater Sci Eng A,* 323 (2002) 251.

14 Mishra R S, Mahoney M W, McFadden S X, Mara N A & Mukherjee A K, *Scr Mater,* 42 (1999) 163.

15 Mahoney M W, Bingel W H, Sharma S R & Mishra R S, *Mater Sci Forum,* 426–432 (2003) 2843.

16 Berbon P B, Bingel W H, Mishra R S, Bampton C C & Mahoney M W, *Scr Mater,* 44 (2001) 61.

17 Sharma V, Prakash U & Kumar B V M, *J. Mater Process Technol,* 224 (2015) 117.

18 Chen C F, Kao P W, Chang L & Ho N J, *Mater Trans,* 51 (2010) 933.

19 Yang M, Xu C, Wu C, Lin K C, Chao Y J & An L, *J Mater Sci,* 45 (2010) 4431.

20 Srinivasan C & Karunanithi M, *J Nanotechnol,* (2015).

21 Salehi M, Farnoush H, Heydarian A & Aghazadeh Mohandesi J, *Metall Mater Trans B Process Metall Mater Process Sci,* 46 (2014) 20.

22 Hosseini S A, Ranjbar K, Dehmolaei R & Amirani A R, *J Alloys Compd,* 622 (2015) 725.

23 Mishra R S & Ma Z Y, *Mater Sci Eng R Reports,* 50 (2005) 1.

24 Azizieh M, Kokabi A H & Abachi P, *Mater Des,* 32 (2011) 2034.

25 Morisada Y, Fujii H, Nagaoka T & Fukusumi M, *Mater Sci Eng A,* 433 (2006) 50.

26 Rathee S, Maheshwari S, Siddiquee A N & Srivastava M, *Mater Today Proc,* 4 (2017) 452.

27 Wang W, Shi Q yu, Liu P, Li H ke & Li T, *J. Mater Process Technol,* 209 (2009) 2099.

28 Asadi P, Faraji G & Besharati M K, *Int. J. Adv Manuf Technol,* 51 (2010) 247.

29 Parumandla N & Adepu K, *Part Sci Technol,* 38 (2020) 121.

30 Chen X G, da Silva M, Gougeon P & St-Georges L, *Mater Sci Eng A,* 518 (2009) 174.

31 Prado R A, Murr L E, Shindo D J & Soto K F, *45* (2001) 75.

32 Vijayavel P, Balasubramanian V & Sundaram S, *Mater Des,* 57 (2014) 1.

33 John J, Shanmuganatan S P, Kiran M B, Senthil Kumar V S & Krishnamurthy R, *Mater Manuf Process,* 34 (2019) 159.

34 Mahmoud E R I, Takahashi M, Shibayanagi T & Ikeuchi K, *Wear,* 268 (2010) 1111.

35 Eftekharinia H, Amadeh A A, Khodabandeh A & Paidar M, *Rare Met,* 39 (2020) 429.
36 Shojaeefard M H, Akbari M, Asadi P & Khalkhali A, *Int J Adv Manuf Technol,* 91 (2017) 1391.
37 Bourkhani R D, Eivani A R & Nateghi H R, *Compos Part B Eng,* 174 (2019) 107061.
38 Singh Yadav R K, Sharma V & Venkata Manoj Kumar B, *Tribol - Mater Surfaces Interfaces,* 13 (2019) 88.
39 Naresh P, Kumar A & Kishore M K, *Mater Sci Forum,* 879 (2017) 1369.
40 Mazaheri Y, Karimzadeh F & Enayati M H, *J Mater Process Technol,* 211 (2011) 1614.
41 Zahmatkesh B & Enayati M H, *Mater Sci Eng A,* 527 (2010) 6734.
42 Rathee S, Maheshwari S, Siddiquee A N & Srivastava M, *Mater Manuf Process,* 33 (2018) 262.
43 Rathee S, Maheshwari S, Siddiquee A N & Srivastava M, *Def Technol,* 13 (2017) 86.
44 Roy P, Singh S & Pal K, *Adv. Compos Mater,* 28 (2019) 1.
45 Jain V K S, Yazar K U & Muthukumaran S, *J Alloys Compd,* 798 (2019) 82.
46 Sarkari Khorrami M, Saito N, Miyashita Y & Kondo M, *Mater Sci Eng A,* 744 (2019) 349.
47 Tang J, Shen Y & Li J, *J Manuf Proces,* 38 (2019) 279.
48 Singh S & Pal K, *J Mater Res Technol,* 8 (2019) 222.
49 Kumar S, *Arch Civ Mech Eng,* 16 (2016) 473.
50 Tonelli L, Morri A, Toschi S, Shaaban M, Ammar H R, Ahmed M M Z, Ramadan R M, El-Mahallawi I & Ceschini L, *Int J Adv Manuf Technol,* 102 (2019) 3945.
51 Huang G, Wu J, Hou W, Shen Y & Gao J, *Mater Manuf Process,* 34 (2019) 147.
52 Sanusi K O & Akinlabi E T, *Mater Tehnol,* 51 (2017) 427.
53 Balakrishnan M, Dinaharan I, Palanivel R & Sathiskumar R, *J Manuf Process,* 38 (2019) 148.
54 Dinaharan I, Balakrishnan M, David Raja Selvam J & Akinlabi E T, *J Alloys Compd,* 781 (2019) 270.
55 Fotoohi H, Lotfi B, Sadeghian Z & Byeon J won, *Mater Charact,* 149 (2019) 124.
56 Lim D K, Shibayanagi T & Gerlich A P, *Mater Sci Eng A,* 507 (2009) 194.
57 Prakrathi S, Ravikumar M, Udupa K R & Udaya Bhat K, *ISRN Mater Sci,* (2013) 1.
58 Manohar P A, Ferry M & Chandra T, *ISIJ Int,* 38 (1998) 913.
59 Kouzeli M & Mortensen A, *Acta Mater,* 50 (2002) 39.
60 Mishra R S, Ma Z Y & Charit I, *Mater Sci Eng A,* 341 (2003) 307.
61 Miranda R M, Santos T G, Gandra J, Lopes N & Silva R J C, *J Mater Process Technol,* 213 (2013) 1609.
62 Kurt A, Uygur I & Cete E, *J. Mater Process Technol,* 211 (2011) 313.
63 Li C, Feng X, Shen Y & Chen W, *Mater Des,* 90 (2016) 922.
64 Singh P, *Experimental Studies on Friction Stir Processing (FSP) and Equal Channel Angular Pressing (ECAP) of Metals and Composites*, Ph D Synopsis, Dayal Bagh Educatioal Institute, Agra, 2018.
65 Thankachan T, Prakash K S & Kavimani V, *Mater Manuf Process,* 33 (2018) 299.
66 Huang Y, Wang T, Guo W, Wan L & Lv S, *Mater Des,* 59 (2014) 274.
67 Raj K H, Sharma R S, Singh P & Dayal A, *Procedia Eng,* 10 (2011) 2904.
68 Girish G & Anandakrishnan V, *Ind Lubr Tribol,* (2020).
69 Aktarer S M, Sekban D M, Yanar H & Purcek G, *IOP Conf Ser Mater Sci Eng,*174 (2017).
70 Vatankhah Barenji R, Khojastehnezhad V M, Pourasl H H & Rabiezadeh A, *J Compos Mater,* 50 (2016) 1457.
71 Yuvaraj N, Aravindan S & Vipin, *J Mater Res Technol,*4 (2015) 398.
72 Ranganathan S, Ramachandran S V, Palanivelu R & Ramasamy S, *SAE Tech Pap,* (2019).
73 Gupta M K, *Carbon Lett,* (2019).
74 Yuvaraj N, Aravindan S & Vipin, *Trans Indian Inst Met,*70 (2017) 1111.
75 Mahmoud E R I, Takahashi M, Shibayanagi T & Dceuchi K, *Mater Trans,* 50 (2009) 1824.
76 Mazaheri Y, Heidarpour A, Jalilvand M M & Roknian M, *J Mater Eng Perform,* 28 (2019) 4826.
77 Mostafapour Asl A & Khandani S T, *Mater Sci Eng A,* 559 (2013) 549.
78 Satish Kumar T, Shalini S & Krishna Kumar K, *Mater Res Express,*7 (2020).
79 Periasamy K, Sivashankar N, Chandrakumar S & Viswanathan R, *Int J Innov Technol Explor Eng,* 9 (2020) 278.
80 Yuvaraj N, *Mater Sci Res India,* 15 (2018) 68.
81 Kishan V, Devaraju A & Prasanna Lakshmi K, *Def Technol,* 13 (2017) 16.
82 Palanivel R, Dinaharan I, Laubscher R F & Davim J P, J Paulo Davim, *Mater Des,* 106 (2016) 195.
83 Rajesh & Kaushik P, *Int J Appl Eng Res,* 12 (2017) 11981.
84 Sert A & Celik O N, *Indian J Eng Mater Sci,* 21 (2014) 35.
85 Akinlabi E T, Mahamood R M, Akinlabi S A & Ogunmuyiwa E, *Adv Mater Sci Eng,* (2014).
86 Nelaturu P, Jana S, Mishra R S, Grant G & Carlson B E, *Mater Sci Eng A,* 716 (2018) 165.
87 Vijayavel P & Balasubramanian V, *Alexandria Eng J,* 57 (2018) 2939.
88 Ikumapayi O M, Akinlabi E T, Pal S K & Majumdar J D, *Procedia Manuf,* 35 (2019) 935.
89 Gupta M K, *SN Appl Sci,* 2 (2020) 1.
90 Veličković S, Garić S, Stojanović B & Vencl A, *Appl Eng Lett,* 1 (2016) 72.
91 Alidokht S A, Abdollah-zadeh A & Assadi H, *Wear,* 305 (2013) 291.
92 Aruri D, Adepu K, Adepu K & Bazavada K, *J Mater Res Technol,* 2 (2013) 362.
93 Rejil C M, Dinaharan I, Vijay S J & Murugan N, *Mater Sci Eng A,* 552 (2012) 336.
94 Dinaharan I, Nelson R, Vijay S J & Akinlabi E T, *Mater Charact,* 118 (2016) 149.
95 Shyam Kumar C N, Bauri R & Yadav D, *Tribol Int,* 101 (2016) 284.
96 Sathiskumar R, Dinaharan I, Murugan N & Vijay S J, *Trans Nonferrous Met Soc China (English Ed),* 25 (2015) 95.
97 Silva F S, *Eng Fail Anal,*13 (2006) 480.
98 Apelian D, *CIRP Encycl Prod Eng,* (2019) 65.

99 Yi J Z, Gao Y X, Lee P D, Flower H M & Lindley T C, *Metall Mater Trans A Phys Metall Mater Sci,*34 A (2003) 1879
100 Lados D A & Apelian D, *Mater Sci Eng A,* 385 (2004) 187.
101 Lados D A & Apelian D, *Mater Sci Eng A,* 385 (2004) 200.
102 Yi J Z, Gao Y X, Lee P D & Lindley T C, *Mater Sci Eng A,* 386 (2004) 396.
103 Lados D A, Apelian D & Donald J K, *Acta Mater,* 54 (2006) 1475.
104 Yi J Z, Gao Y X, Lee P D & Lindley T C, *Metall Mater Trans B Process Metall Mater Process Sci,* 37 (2006) 301.
105 Lados D A & Apelian D, *Eng Fract Mech,*75 (2008) 821.
106 Sharma S R, Ma Z Y & Mishra R S, *Scr Mater,* 51 (2004) 237.
107 Hussein W & Al-Shammari M A, *IOP Conf Ser Mater Sci Eng,* 454 (2018).
108 Sun N, Jones W J & Apelian D, *Int J Met,* 13 (2019) 244.